Title

Simulation Analysis of the Effect of Beam Pipes and Multi-mode Competition in the Standing-wave Free-Electron Laser Two-Beam Accelerator

Author

Wang, C.

Publication Date

1993-11-01

LBL-35122
UC-414
Preprint

Lawrence Berkeley Laboratory
UNIVERSITY OF CALIFORNIA

Accelerator & Fusion
Research Division

Submitted to Nuclear Instruments and
Methods in Physics Research A

Simulation Analysis of the Effect of Beam Pipes and Multi-Mode Competition in the Standing-Wave Free-Electron Laser Two-Beam Accelerator

C. Wang

November 1993

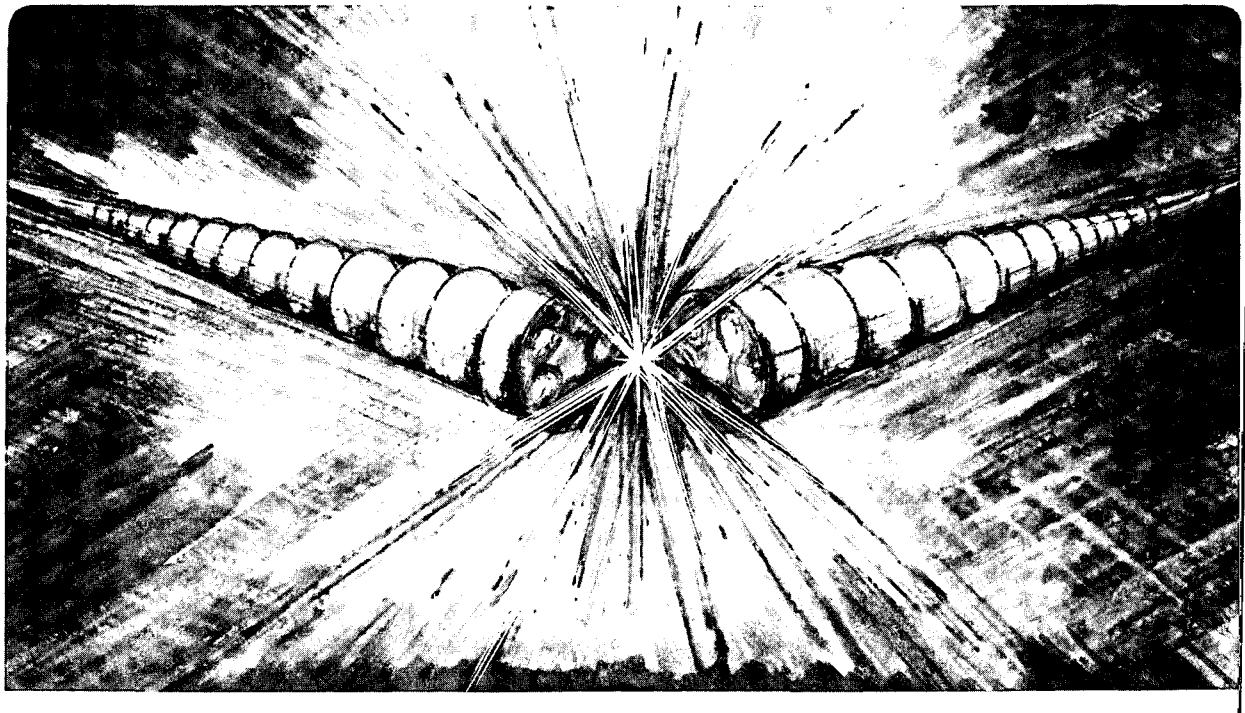

Prepared for the U.S. Department of Energy under Contract Number DE-AC03-76SF00098

DISCLAIMER

LBL-35122
UC-414

Simulation Analysis of the Effect of Beam Pipes and Multi-Mode Competition in the Standing-Wave Free-Electron Laser Two-Beam Accelerator

Changbiao Wang

Center for Beam Physics
Accelerator and Fusion Research Division
Lawrence Berkeley Laboratory
University of California
Berkeley, California 94720

November 1993

This work was supported by the Director, Office of Energy Research, Office of Basic Energy Sciences, Materials Sciences Division, of the U.S. Department of Energy under Contract No. DE-AC03-76SF00098.

Simulation analysis of the effect of beam pipes and multi-mode competition in the standing-wave Free-Electron Laser Two-Beam Accelerator

Changbiao Wang[1]

Center for Beam Physics, Accelerator and Fusion Research Division

Lawrence Berkeley Laboratory, University of California, Berkeley, California 94720

29 November 1993

In this paper, we present simulation results of an array of standing-wave free-electron lasers (SWFELs) in the Standing-Wave Free-Electron Laser Two-Beam Accelerator (SWFEL/TBA) configuration. The influence of betatron motion on the stability of rf output energy is analyzed. The effects of beam pipes and finite emittance on rf output power are examined, and investigation is made of possible of mode competition. It is shown that for an array of SWFELs with 9 cavities and a 100.6-ns, 0.5-kA, 7.98-MeV, 2.0×10^{-4}-π m normalized-emittance electron beam, prebunched at 17.1 GHz, an averaged energy output of 12.3J/m can be obtained with a fluctuation of less than 6.5%. It is also shown that potential competitive longitudinal modes can be suppressed by inserting irises along the electric field direction at some node points of the electric field of the operating mode.

[1]Permanent address: High Energy Electronics Research Institute, University of Electronic Science and Technology of China, Chengdu, Sichuan 610054, China

1. Introduction

In the future TeV-class linear colliders, rf power of above 100MW/m with a pulse length of 50-100 nsec is required to drive a high-gradient traveling-wave accelerator structue of 100MeV/m in a frequency range of 10-30 GHz [1]. It has been demonstrated experimentally that the relativistic klystron (RK) and the free-electron laser (FEL) are all high-power rf devices [2,3], and they were proposed as rf sources in the Two-Beam Accelerator (TBA) [4,5]. A great deal of work has been done on the Standing-Wave Free-Electron Laser Two-Beam Accelerator (SWFEL/TBA) [1,6-12] using the continuum-cavity model [1,6,7], the discrete-cavity model [8,9], and the impedance-based analysis method [10]. Those treatments are all based on a one-dimensional assumption. Recently, a three-dimensional simulation analysis has been made to investigate a multi-cavity FEL without reacceleration cells between cavities[11]. Further, work was done on an array of standing-wave free-electron lasers (SWFELs) in the SWFEL/TBA configuration, which has 9 FEL sections, each with its own reacceleration cell [12]. It indicated that the phase-space distribution before each cavity becomes quite similar, and a stable energy output can be obtained by setting the length of the FEL section equal to an integer multiple of the wiggler period. In that work, however, the cavity eigen mode field was taken to be that of an ideal rectangular cavity and the effect of beam pipes was neglected. How much effect the pipes have is a significant problem.

Any electron beam has finite emittance and the emittance results in an effective energy spread. The energy spread of a beam can be phenomenologically divided into two parts (see Eq. (4)): one is related to the transverse emittance and the other is related to the longitudinal emittance (which corresponds to the axial energy spread). In this sense, the transverse emittance makes an additional effective energy spread as well as increasing the beam's effective radius. In our previous work [12], the transverse emittance effects on the energy spread and the beam radius were neglected. The energy spread affects the FEL interaction. To decrease the influence of pipes, we want as small a pipe radius as possible.

How the transverse emittance affects rf energy output and whether it causes electrons to be intercepted by the pipes need to be examined.

In the present version of SWFEL/TBA, the SWFEL operates in a high-order mode, and the problem of multi-mode competition may arise. As it is well-known, the bandwidth of a cavity is $1/2Q_t$ [13],with Q_t the total cavity quality factor, and the FEL gain bandwidth is of the order of $1/N_w$ [14], with N_w the wiggler period number. To obtain stable power output from a cavity, usually the quality factor is not very high. For example, the cavity bandwidth is up to about 3% for a quality factor of 16. The gain bandwidth is much larger, up to about 17% for a FEL section with six wiggler periods. For a SWFEL operating in $TE_{0,1,96}$ mode [12], however, the transverse-mode frequency spacing is about 7% and the longitudinal-mode frequency spacing is only about 1%. So the FEL radiation field may excite several longitudinal modes although the unwanted transverse modes can be easily suppressed. It is not appropriate to increase the wiggler period number to narrow the gain bandwidth and suppress those undesired longitudinal modes. That is because for a given operating frequency it will cause some other problems such as decrease of the input beam power and increase of the transverse gradient effect of the wiggler field. Hence, to determine what modes are potential competitive modes and determining how to suppress those undesired modes is an important problem.

In this work, based on our previous one [12], we present simulation results of the effects of beam pipes and finite transverse emittance on rf output power, and the interaction of an electron beam with different longitudinal modes in an array of SWFELs of the SWFEL/TBA configuration. It is shown that for $TE_{0,1,96}$ mode the electric field is rapidly cut off within the pipes when the pipe height is not larger than one fifth of the cavity height. For a 100.6-ns, 0.5-kA, 7.98-MeV, 2.0×10^{-4}-π m normalized-emittance electron beam prebunched at 17.1 GHz, all the electrons can pass through the SWFELs, and an averaged energy output of 12.3J/m can be obtained with a fluctuation of less than 6.5%. It is also

shown that potential competitive longitudinal modes can be suppressed by inserting irises along the cavity wide side at some node points of the electric field of the $TE_{0,1,96}$ mode.

The paper is organized as follows. In Sec. 2, the pipe effect on $TE_{0,1,96}$ mode in an ideal rectangular cavity is examined with the help of MAFIA. In Sec. 3, the effects of betatron motion on axial velocity spread and variations of output energy is analyzed. Sec. 4 is devoted to examine the effect of beam pipes and transverse emittance on rf output power, and investigate the interaction of an electron beam with different longitudinal modes to determine potential competitive modes. In Sec.5 a scheme of suppressing competitive modes is proposed, and finally, in Sec. 6 some remarks are given.

2. Effect of beam pipes on the operating-mode field in an ideal FEL cavity

MAFIA [15] is extensively used to calculate rf cavities in the accelerator community, but typically only those cavity modes with fairly small mode indices are involved [16]. In the SWFEL/TBA configuration, however, the FEL interaction cavity is rather long and it contains up to 96 half wavelengths [12]. It can be shown by direct analysis that there are 1335 TE modes and 721 TM modes, for a rectangular cavity with width 5 cm, height 3 cm, and length 86.89 cm, before the $TE_{0,1,96}$ mode. From this it seems impossible to use MAFIA to compute the effect of pipes on a FEL cavity because it will take too much computer time, and the accuracy of the result we would obtain is also questionable. Here we present a technique of approximate calculation for this situation.

The array of SWFELs used in the simulation has 9 FEL sections which are the same, each with a rectangular cavity (5 cm wide and 3 cm high), two pipes, and a reacceleration cell. The FEL section, as shown in Fig. 1, has a length of 102 cm (six wiggler periods), and the cavity together with pipes has a length of 95.96 cm. In an ideal case, the FEL operates in the $TE_{0,1,96}$ mode and there is no field in the pipes. But in practice, introduction of the pipes destroys the boundary conditions for an ideal cavity, and the

cavity field will be changed. Our purpose is to determine how much effect the pipes have when the pipe transverse dimensions are reasonably small.

From electromagnetic theory, we know that inserting a metal plane at the electric-field node point of a resonant mode in a cavity will not change the field distribution of the mode. To use MAFIA to calculate the pipe effect, the cavity together with the two pipes is divided into three parts: two end cavities, which are the same, and one middle cavity (see Fig. 1). The eigen field data for a modified $TE_{0,1,1}$ mode in the end cavity are obtained through MAFIA, and the field data in the middle cavity come from an ideal rectangular cavity operating in the $TE_{0,1,94}$ mode with the same resonant frequency as the end cavity. Obviuosly, this is an approximation because we have implicitly assumed that introduction of pipes only modifies the field of the end cavities whereas the field of the middle cavity is kept unchanged. In principle, the method has a enough accuracy if the field in the pipes is rapidly cut off.

Running MAFIA indicates that when the pipe height is less than 6 mm the $TE_{0,1,1}$ mode is cut off within a half waveguide wavelength in the pipe. The pipe width has a less important effect because the rf induction current of the mode flows along the x-direction on the wall which connects the pipe and the cavity. Considering that electrons in the wiggler field move along the x-direction in the range about from -1.5 cm to 1.5 cm, we take the pipe width as 4 cm. A oversmall-height pipe is not helpful to the passage of an electron beam and the height is taken as 6 mm. Figure 2 shows the end cavity used in the simulation and figure 3 shows its electric field pattern on a symmtric plane of y=0.

From MAFIA we can get electric and magnetic field data which are not normalized. To use these data in the code RKFEL [12], we have to normalize them. Considering that the eigen electric field and vector potential are different by a drive angular frequency, we obtain the vector-potential normalizing coefficient

$$NA = \int_{\text{middle cavity}} \mathbf{A} \cdot \mathbf{A}\, d^3\mathbf{x} + \int_{\text{end cavities}} \mathbf{A} \cdot \mathbf{A}\, d^3\mathbf{x} \qquad (1)$$

where **A** stands for the vector potential. The field data of the first part in the above expression come from an analytical formula for the $TE_{0,1,94}$ mode mentioned previously, and the ones of the second part come from MAFIA. After the code RKFEL reads in the normalezed field data from MAFIA, we can obtain the on-axis dependence of the vector potential A_x on axial distance in the first cavity including pipes, as shown in Fig. 4. From this we find that the pipe effect behaves as if the original interaction region were prolonged a little.

3. Betatron effect on axial velocity spread

In the FEL interaction, when an electron which is synchronous with the radiation wave passes through a wiggler period along the axial direction, the wave travels one wavelength ahead of the electron [17]. From this it follows that the axial velocity spread of an electron beam will widen the radiation spectrum and degrade coherence. Consequently, the gain of a FEL strongly depends on the axial velocity spread. Here we will examine the effect of equilibrium betatron motion of a no-transverse emittance electron beam on the axial velocity spread. The parameters of the beam and the wiggler field are given in table 1.

As is well-known, betatron motion results from the transverse gradient effect of a wiggler field. The vector potential of the linear wiggler magnetic field used in the simulation, provided by parabolically curved magnet pole faces, is given by the following analytic expression

$$A_x = T(z)\frac{B_{w0}}{k_w}\,\mathrm{ch}(k_x x)\,\mathrm{ch}(k_y y)\,\sin(k_w z), \tag{2}$$

$$A_y = -T(z)\frac{B_{w0}}{k_w}\frac{k_x}{k_y}\,\mathrm{sh}(k_x x)\,\mathrm{sh}(k_y y)\,\sin(k_w z), \tag{3}$$

where B_{w0} is the wiggler magnetic field amplitude on the axis, the wiggler wave number is given by $k_w=2\pi/\lambda_w$ with λ_w the wiggler period, $kx^2+ky^2=k_w^2$, and the tapering factor is given by $T(z)=z/7\lambda_w$ when $z<7\lambda_w$, and $T(z)=1$ when $z\geq 7\lambda_w$.

Scharlemann [18] showed that in the linear wiggler described by Eqs.(2) and (3), the axial velocity of an individual electron, averaged over a wiggler period, is not modulated by the betatron motion of the electron. On different betatron orbits, however, electrons have different betatron velocities, and the betatron motion will modulate axial velocities and axial velocity spread. Figure 5 shows the relation between the rms-normalized axial velocity spread for a buchet of beam with 200 computational particles and the betatron motion in the y-direction for a representative particle from the buchet. From it we clearly find that the velocity spread oscillates with the electron's wiggler motion and the oscillations are modulated with a period of the half betatron period. Simulations indicate that when the length of each FEL section is equal to an integer multiple of the wiggler period and the half betatron period, the output energy from cavities is the most stable. That is because, for this geometry, we have greatly reduced the asymmetry of the equilibrium phase space caused by the betatron motion when an electron beam passes through each FEL section. For the parameters used in the simulation, the betatron period $\lambda_{\beta y}$, from a analytic calculation by using the formula $\lambda_{\beta y}=2\sqrt{2}\pi\gamma/(a_w k_y)$ [18] with γ the electron's relativistic factor and a_w the wiggler parameter, is 78.4 cm, whereas the simulation result is 68 cm, 4 times the wiggler period. So the length of the FEL section is taken as 102 cm, 3 half betatron periods or 6 wiggler periods.

The oscillations of the velocity spread with wiggler motion can be qualitatively explained as follows. Suppose that we have a single-energy electron beam with only two electrons. The transverse wiggler velocity is proportional to $a_{wi}\sin(k_w z)$, (i =1,2), where a_{wi} is the electron's effective wiggler parameter. Due to the wiggler transverse gradient effect, a_{w1} is different from a_{w2}. The transverse rms-velocity spread for the beam is $|0.5(a_{w1}-a_{w2})\sin(k_w z)|$. When $\sin(k_w z)=0$, the transverse velocity spread is equal to zero and the axial velocity spread is also equal to zero. When $|\sin(k_w z)|=1$, the transverse velocity spread reaches its maximum and the axial velocity spread also reaches its maximum. So the axial velocity spread oscillates with the electron's wiggler motion.

From Fig. 5 we find that at the nodes of the velocity spread the spread is not zero because the beam has an initial axial energy spread and executes betatron motion.

Although making use of the periodicity of betatron motion, and a proper choice of the length of a FEL section, can greatly reduce the asymmetry of the phase space, we can not eliminate the effect competely. Figure 6 shows the dependence of betatron velocity in the y-direction on axial distance when the representative electron mentioned above travels through FEL sections 1, 5, and 9. We find that the betatron period is the same but the details within different periods are a little different. So the betatron motion is quasi-periodic.

4. Simulation results

We have simulated the array of SWFELs using the parameters given in table 1. It is assumed that a well-bunched beam has been formed before it enters the wiggler field described by Eqs.(2) and (3). The simulation particle initialization parallels the bunched beam. There are 87 buchets in a 100.6-ns pulse beam, and the interval between adjacent buchets is 20 periods of the 17.1-GHz drive wave. Each bunch has 200 computational particles and they are uniformly distributed in a phase spread of 0.2π.

The transverse emittance effect on the energy spread is taken into account in the RKFEL code through the following model

$$(\Delta\gamma)_t = (\Delta\gamma)_z + \frac{0.5\gamma_0\varepsilon_n^2}{\beta_0^2 r_b^2} \tag{4}$$

where $(\Delta\gamma)_t$ is the total energy spread, $(\Delta\gamma)_z$ is the initial axial energy spread caused by the longitudinal emittance, γ_0 and β_0 are, respectively, the central relativistic factor and normalized total velocity of the input beam, ε_n is the normalized transverse emittance, and r_b is the beam's radius. The second term on the right-hand side of Eq. (4) is the additional effective energy spread made by the transverse emittance. The 200 computational particles

are randomly distributed in the x-β_x and y-β_y phase ellipses with the major axis r_b and the minor axis $\varepsilon_n/(\gamma_0\beta_0 r_b)$.

4.1 Pipe and emittance effects on FEL energy output

In order to examine the pipe and transverse emittance effects, we will take three cases. In the first case, both the emittance and pipe effects are taken into account. The normalized emittance is 2.0×10^{-4} π m and an eigen mode field modified by the beam pipes, described in Sec. 2, is employed. In the second case, only the pipe effect is considered. The emittance is taken as zero and the modified eigen mode field is used. In the third case, no pipe and no emittance effects are considered. The emittance is zero and the eigen mode field comes from an ideal rectangular cavity with a length of 86.89 cm, operating in the $TE_{0,1,96}$ mode.

Figure 7 shows the dependence of output energy on cavity number for the three cases. For the first case, the averaged output energy is 12.3 J/m with a fluctuation of less than 6.5%. For the second case the averaged output energy is 13.2 J/m and the fluctuation is less than 6.0%. For the third case, the averaged output energy is 12.8 J/m and the fluctuation is less than 6.2%. Comparing the first case with the second case, we find that the emittance reduces the output energy and increases fluctuations. That is because the emittance makes initial transverse velocities and an additional effective energy spread, resulting in increase of the axial velocity spread when the beam passes through the wiggler. Simulation result also indicates that all the electrons have passed through the 9 FEL sections when the normalized emittance is less than 2.0×10^{-4} π m. Comparing the second case with the third case, we see that the pipe effect makes the output energy increase a little because the effective interaction region is longer than that with no pipe effect, as mentioned in Sec. 2.

Figure 8 shows the output power versus time from representative cavities 1, 5 and 9 for the first and third cases. The maximum power difference is less than 12.5% for the flat

part. From Fig. 7, the averaged output energy is only different by 4% between the first and third cases. Therefore, ignoring influence of beam pipes and emittance is a good approximation when the emittance and the transverse dimensions of pipes are small enough.

Figure 9 shows the dependence of output power on cavities 1, 5, and 9 for the first case. From it we find that the rf output pulses extracted from the cavities becomes a little shorter with increase in cavity number. This pulse shortening phenomenon can be explained as follows. The input beam has an axial velocity spread and the spread trends to debunch the beam when it is travelling [19]. However, the FEL interaction has the effect of constraining the phase spread [12]. Before the first bunch goes into the array of SWFELs, there is no rf field in all the FEL cavities. When the bunch travels through the cavities, an rf field is set up. Due to the debunching effect of the velocity spread, however, the rf current decreases along the beam direction, and so the rf fields excited in the cavities also decrease in strength along the beam direction. With the subsequent bunches travelling through the cavitites one by one, the rf field in each cavity grows, but the field in the cavity at which the beam arrives first grows faster than that in the cavity at which the beam arrives later. When the rf field arrives at a stable state, the phase-constraining effect of the FEL interaction almost cancels the debuching effect of the velocity spread, and so essentially the same rf field is excited in each cavity. But it takes a longer time for the rf field to arrive at a stable state in the cavity that the beam reaches later, which results in the rf pulse shortening phenomenon.

To confirm the above analysis, we ran the code using a beam with only one particle per bunch. This is an ideal prebunched beam without any axial velocity spread. For this case the rf pulse shortening phenomenon does not appear any more.

4. 2 Potential competitive modes

As indicated above, ignoring the pipe and emittance effects is a good approximation when they are small enough. We will investigate the interaction of an electron beam with different modes by neglecting the pipe and emittance effects to find out what modes are potential competitive modes. The parameters are exactly the same as those in the third case above. The operating mode is $TE_{0,1,96}$ and what we are most concerned about is those longitudinal modes in the vicinity of the operating mode, because they have close resonant frequencies.

Figure 10 shows the dependence of rf output energy on cavity number when the beam interacts with $TE_{0,1,93}$, $TE_{0,1,94}$, $TE_{0,1,95}$, $TE_{0,1,96}$, and $TE_{0,1,97}$ modes respectively. From it we see that for $TE_{0,1,93}$, and $TE_{0,1,97}$ modes, the cavities have almost no energy output and therefore can not compete with the operating mode. For $TE_{0,1,94}$ and $TE_{0,1,95}$ modes, however, the cavities have considerable output energy, and especially for $TE_{0,1,95}$ mode, the output energy in the first cavity is much larger than the operating mode. Hence they are potential competitive modes.

In the SWFELs, the radiation wave is required to fulfil two conditions. One is the cavity resonant condition that the cavity frequency detuning $|(\omega-\omega_0)/\omega_0|$ should be less than the cavity bandwidth, where ω is the drive wave frequency and ω_0 is the cavity resonant frequency. The other one is the FEL resonant condition that the FEL frequency detuning $[(k_w+k_z)\langle v_z\rangle-\omega]/\omega$ should be less than the gain bandwidth, where k_z is the wave number of radiation wave and $\langle v_z\rangle$ is the averaged axial velocity of a beam over one wiggler period. According to one-dimensional small signal gain theory [20], the FEL gain is maximized when $[(k_w+k_z)\langle v_z\rangle-\omega]=2.61\langle v_z\rangle/L_c$, where L_c is the cavity length. In our situation, $\langle v_z\rangle=0.945c$ with c the light speed in free space, L_c=0.8689 m, and ω=107.442×10^9 sec^{-1}, and we obtain an analytic optimum FEL frequency detuning of 0.79%. The simulation result is about 1.26%. By considering that our wiggler field is three-dimensional, the result is quite reasonable.

The less the cavity frequency detuning is, the more strongly an rf field can be set up for the same excitation in a cavity. The less the FEL frequency detuning deviates from its optimum, the stronger is the FEL function of constraining the phase spread, which effectively keeps a beam bunched. So cavity and FEL frequency detunings have a great effect on axial velocity spread and variations of output energy with cavities. The two detunings for different modes are given in table 2. Figures 11 and 12 show the dependence of rms-normalized axial velocity spread on axial distance for different modes within the second and the ninth FEL sections respectively. For the $TE_{0,1,97}$ mode, the spread curve overlaps the one without rf field because the mode has a large cavity detuning and it does not have a very strong rf field set up in the cavities. $TE_{0,1,95}$ mode has the least cavity detuning but its FEL detuning has a larger deviation. Although the mode has a very strong rf field in the first few cavities, the effect of constraining the phase spread is not so strong during the interaction that it badly increases axial velocity spread, and its output energy rapidly decreases with cavity number.

The cavity detuning of the operating mode $TE_{0,1,96}$ is a little larger than the one of the $TE_{0,1,94}$ mode but its FEL detuning has an optimum value. So the axial velocity spread for the operating mode is smaller, and its output energy is bigger and much more stable. For $TE_{0,1,93}$ mode, both the cavity detuning and the deviation of the FEL detuning are very large and the spread curve also overlaps the one without rf field. It should be noted that although the FEL detuning for $TE_{0,1,94}$ mode is a little less than zero the mode still has an rf output energy because the electron beam used in the simulation is a prebunched beam.

5. Mode suppresion

We have found out that the $TE_{0,1,94}$ and $TE_{0,1,95}$ modes are the potential competitive modes. Now the problem we have to solve is how to suppress these undesired modes.

According to electromagnetic theory, any possible electromagnetic mode in a resonator has definate boundary condition. If the boundary condition is essentially destroyed, then

the mode will not exist any more. Based on the above idea, we propose a suppression scheme of these potential competitive modes, as shown in Fig. 13. From it we can see that the points at $0.5d$, and $0.25d$ and $0.75d$ in a $TE_{0,1,96}$-mode cavity with a length of d are standing-wave nodes of the electric field of the mode but they are peaks of $TE_{0,1,95}$ ($TE_{0,1,97}$) mode and $TE_{0,1,94}$ ($TE_{0,1,98}$) mode respectively. So if we insert irises along the x-direction, (the electric field direction), then the electric fields for the competitive modes are short-circuited and they can not exist. For the operating mode, however, the boundary condition actually is not changed and the mode field will be unaffected.

Unfortunately, we can not use MAFIA to directly confirm the above scheme because MAFIA is not good at calculating very high-order modes. But we have made a principle-proof for a short rectangular cavity using MAFIA. When no irises are inserted, the cavity can support $TE_{0,1,1}$ mode with a resonant frequency of 9.6 GHz and $TE_{0,1,2}$ mode with a resonant frequency of 17.1 GHz. Then we insert irises at the middle point along the electric field direction and run MAFIA again. We find that $TE_{0,1,1}$ mode does not exist any more but $TE_{0,1,2}$ mode is still there, as shown in Fig. 14.

6. Remarks

We have simulated the interaction of a 0.5-kA, 7.98-MeV electron beam prebunched at 17.1 GHz with $TE_{0,1,96}$ mode in an array of SWFELs, with the pipe and transverse emittance effects taken into account. By setting the length of each FEL section as an integer multiple of the wiggler period and the half betatron period to reduce variations of output energy from cavity to cavity, a stable output energy with an average of 12.3 J/m and a fluctuation of less than 6.5% has been obtained. Intrinsic finite emittance and energy spread, and transverse variations of the wiggler field are all the source of axial velocity spread for an equilibrium electron beam [22]. The axial velocity spread has an effect of debunching and the FEL interaction has an effect of constraining the phase spread. The velocity spread is responsible for rf output pulse shortening along the beam direction in the

array of SWFELs. Simulations indicates that $TE_{0,1,94}$ and $TE_{0,1,95}$ modes are potential competitive modes and they can be suppressed by placing irises at the standing-wave nodes of the electric field of the operating mode.

Nevertheless, there is still a lot of work we must do. An important effect, for example, the space charge effect is not considered in this simulation, and nor is the effect of beam breakup (BBU) instability [21]. In addition, the axial velocity spread is very sensitive to the FEL interaction as we have seen. In principle, if the effect of constraining the phase spread can exactly cancel the effect of debunching caused by the velocity spread, then the spread will be kept in a small range and a stable energy output can be obtained in a very long array of SWFELs. There are many factors related to the spread. Therefore, under what conditions the axial velocity spread can be confined in a small range is still an interesting theoretical problem in the SWFEL/TBA configuration.

Acknowledgements

The author would like to thank A. M. Sessler for his careful review of this paper. The author also wishes to thank D. H. Whittum and Hai Li for their useful discussions, and R. A. Rimmer, F. Krawczyk, and K. Ko for their help in using MAFIA. The work was supported by the Director, Office of Energy Research, Office of High Energy and Nuclear Physics, Division of High Energy Physics, of the U. S. Department of Energy under Contract No. DE-AC03-76SF00098.

Table 1

Parameters in the simulation

Magnetic wiggler parameters	
Wiggler period	17 cm
Wiggler amplitude on axis	0.455 T
Wiggler parameter	7.22
Wiggler wave number	36.960 m^{-1}
k_x (=k_y)	26.134 m^{-1}
Tapered wiggler period number	7
Beam parameters	
Beam central energy	7.982 MeV
Central relativistic factor γ_0	16.62
Beam radius	2.5 mm
Beam current	500 A
Beam initial phase spread	0.2π
Beam initial axial energy spread $(\Delta\gamma)_z/\gamma_0$	2%*
Pulse length	100.6 ns
Pulse rise time (=fall time)	4.7 ns
Structure parameters	
Reacceleration cell length	6.04 cm
Cavity length (including pipes)	95.96 cm
Cavity transverse dimension (width×height)	5 cm×3 cm
Wall-dissipation quality factor	10000
External quality factor	16
Others	
Drive frequency	17.1 GHz
FEL section number	9
FEL section length	102 cm

*In Ref. 12, the energy spread is defined as the difference between the maximum energy and the central energy in the beam. Here it is defined as the differece between the maximum energy and the minimum energy.

Table 2

Cavity frequency detuning and FEL frequency detuning for different modes

mode	resonant frequency	cavity detuning	FEL detuning
$TE_{0,1,93}$	16.803 GHz	1.8%	-1.6%
$TE_{0,1,94}$	16.968 GHz	0.8%	-0.64%
$TE_{0,1,95}$	17.133 GHz	0.2%	+0.31%
$TE_{0,1,96}$	17.298 GHz	1.1%	+1.26%
$TE_{0,1,97}$	17.464 GHz	2.1%	+2.22%

References

1 A. M. Sessler, D. H. Whittum, J. S. Wurlete, W. M. Sharp, and M. A. Makowski, Nucl. Instr. and Meth. A306 (1991) 592.

2 M. A. Allen, J. K. Boyd, R. S. Callin, H. Deruyter, K. R. Eppley, K. S. Fant, W. R. Fowkes, J. Haimson, H. A. Hoag, D. B. Hopkings, T. Houck, R. F. Koontz, T. L. Lavine, G. A. Loew, B. Mecklenburg, R. H. Miller, R. D. Ruth, R. D. Ryne, A. M. Sessler, A. E. Vlieks, J. W. Wang, G. A. Westenskow, and S. S. Yu, Phys. Rev. Lett. 63(1989) 2472.

3 T. J. Orzechowski, B. R. Anderson, J. C. Clark, W. M. Fawley, A. C. Paul, D. Prosnitz, E. T. Scharlemann, S. M. Yarema, D. B. Hopkins, A. M. Sessler, and Wurtele, Phys. Rev. Lett. 57 (1986) 2172.

4 A. M. Sessler and S. S. Yu, Phys. Rev. Lett. 58 (1987) 2439.

5 A. M. Sessler, Proc. Workshop on the Laser Acceleration of Particles, eds. C. Joshi and T. Katsouleas, AIP Conf. Proc. 91 (1982) 154.

6 W. M. Sharp, A. M. Sessler, D. H. Whittum, and J. S. Wurlete, Nucl. Instr. and Meth. A304 (1991) 487.

7 W. M. Sharp, G. Rangarajan, A. M. Sessler, and J. S. Wurlete, Proc. SPIE Conference 1407 (1991) 535.

8 G. Rangarajan and A. M. Sessler, Proc. Advanced Accelerator Concepts, ed. J. S. Wurtele, AIP Conf. Proc. 279 (1992) 156.

9 G. Rangarajan, A. M. Sessler, and W. M. Sharp, Nucl. Instr. and Meth. A318 (1992) 745.

10 J. S. Wurtele, D. H. Whittum, and A. M. Sessler, Proc. Advanced Accelerator Concepts, ed. J. S. Wurtele, AIP Conf. Proc. 279 (1992) 143.

11 C. Wang and A. M. Sessler, Proc. Intense Microwave Pulse, ed. H. E. Brandt, SPIE 1872 (1993) 130.

12 C. Wang and A. M. Sessler, to be published in Proc. 1993 PAC, Lawrence Berkeley Laboratory Report LBL-33256, May, 1993.

13 R. E. Collin, Foundations for Microwave Engineering, p.314, McGraw-Hill Book Company, NY, 1966.

14 C. A. Brau, Free-Electron Lasers, p. 107, Academic Press, San Diego, 1990.

15 F. Ebeling, R. Klatt, F. Krawczyk, E. Lawinsky, S. G. Wipf, T. Weiland, T. Barts, M. J. Browman, R. K. Cooper, G. Rodenz, and B. Steffen, Mafia User Guide, Los Alamos National Laboratory Report LA-UR-90-1307, 1989.

16 R. Govil, R. A. Rimmer, A. M. Sessler, and H. G. Kirk, Nucl. Instr. and Meth. A331 (1993) 335.

17 P. L. Morton, Phys. Quan. Elect. 8 (1982) 1.

18 E. T. Scharlemann, J. Appl. Phys. 58 (1985) 2154.

19 C. Wang, submitted to Fifth Special Issue on High Power Microwaves of the IEEE Transactions on Plasma Science, Lawrence Berkeley Laboratory Report LBL-34513, August 1993.

20 T. C. Marshall, Free-Electron Lasers, p. 52, Macmillan Publishing Company, NY, 1985.

21 J. S. Kim, H. Henke, A. M. Sessler, and D. H. Whittum,to be published in Proc. 1993 PAC, Lawrence Berkeley Laboratory Report LBL-33255, May, 1993.

22 This can be seen from the following qualitative explanation. Suppose that the dimension of transverse motion of an individual electron is so small that the one-dimensional linear wiggler model holds. Then the electron's normalized axial velocity, averaged over a wiggler period, can be written as $\beta_z=1-0.5(1+P_\perp^2+0.5a_{we}^2)/\gamma^2$, where a_{we} is the effective wiggler parameter, $\gamma$is the electron's normalized energy, and $P_\perp$ is the normalized transverse canonical momentum, which is decided by the initial transverse velocity and energy. Due to the gradient effect of the wiggler, different electrons have different effective wiggler parameters. Due to the emittance and energy spread, these electrons have different initial transverse velocities and energy. From this it follows that the axial velocity spread is related to the emittance, energy spread, and the gradient effect of the wiggler. It should be noted that the wiggler transverse variations have two ways to affect the axial velocity spread: one is through changing the effective wiggler parameter just as mentioned above, and the other is through setting up an additional axial magnetic field and resulting in betatron motion, which is not considered above but we have seen in Sec.3.

Figure Captions

Fig. 1 A FEL section.

Fig. 2 End cavity dimensions.

Fig. 3 Modified $TE_{0,1,1}$-mode electric field pattern on the y-symmetric plane in the end cavity.

Fig. 4 Dependence of the on-axis normalized vector potential A_x on axial distance in the first cavity including pipes. Solid curve: with pipe effect, and dashed curve: without pipe effect. The field is rapidly cut off within pipes.

Fig. 5 Betatron-motion modulation of axial velocity spread for a buchet of beam with a central energy of 7.98 MeV. Upper: rms-normalized axial velocity spread versus axial distance in the first two FEL sections, middle: normalized betatron velocity in the y-direction versus axial distance for a representative electron with γ=16.647 in the beam, and lower: betatron displacement of the electron.

Fig. 6 Normalized betatron velocity versus FEL section axial distance in the first, fifth, and ninth FEL sections for the representative electron. Betatron motion is quasi-periodical.

Fig. 7 Dependence of output energy on cavity number for three different cases. Case 1: normalized transverse emittance is 2.0×10^{-4} π m and pipe effect is taken into account. Case 2: no emittance but pipe effect is included. Case 3: no emittance and no pipe effect are considered.

Fig. 8 Dependence of output power on time for case 1 and case 3. Due to the emittance effect, the output power is decreased a little, especially for the ninth cavity.

Fig. 9 Dependence of output power on time for case 1. Along the beam direction, the rf output power pulse is shortened. This pulse shortening phenomenon is caused by the effect of debunching.

Fig. 10 Dependence of output energy on cavity number for different longitudinal modes. The potential competitive modes are $TE_{0,1,94}$ and $TE_{0,1,95}$ modes.

Fig. 11 Dependence of rms-normalized axial velocity spread on axial distance for different modes in the second FEL section. Thick curve: spread in the absence of rf field, and thin curve: spread in the presence of rf field. Competitive modes have larger axial velocity spreads.

Fig. 12 Dependence of rms-normalized axial velocity spread on axial distance for different modes in the ninth FEL section. Compared with competitive modes, the operating mode $TE_{0,1,96}$ has a much smaller spread.

Fig. 13 A suppression scheme of potential competitive modes. At $0.5d$ placing irises along the electric field direction can suppress $TE_{0,1,95}$ and $TE_{0,1,97}$ modes. At $0.25d$ or $0.75d$ placing irises can suppress $TE_{0,1,94}$ and $TE_{0,1,98}$ modes.

Fig. 14 Electric field pattern for $TE_{0,1,2}$ mode from MAFIA. When irises are placed at the cavity middle along the electric field direction, $TE_{0,1,1}$ no longer exists.

Fig. 1

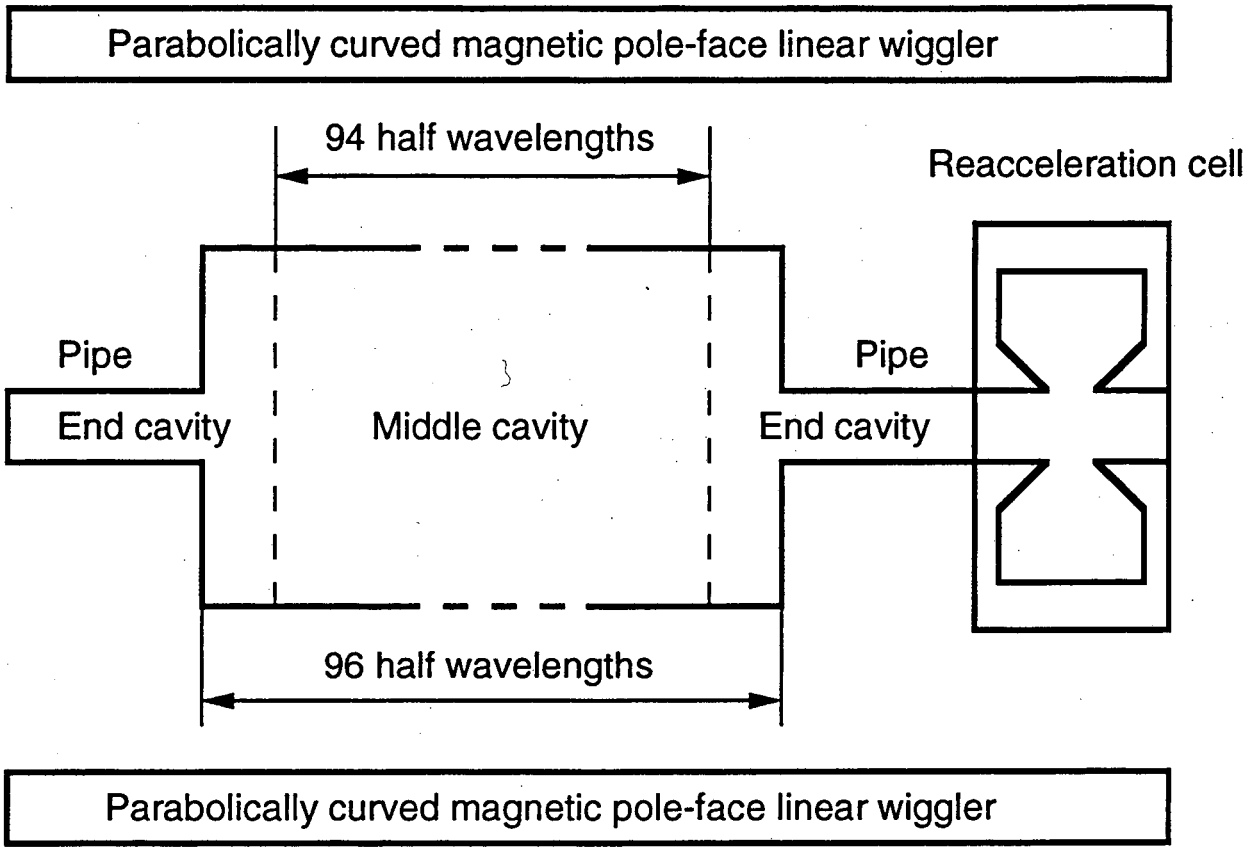
Parabolically curved magnetic pole-face linear wiggler
94 half wavelengths
Reacceleration cell
Pipe
End cavity
Middle cavity
Pipe
End cavity
96 half wavelengths
Parabolically curved magnetic pole-face linear wiggler

Fig. 2

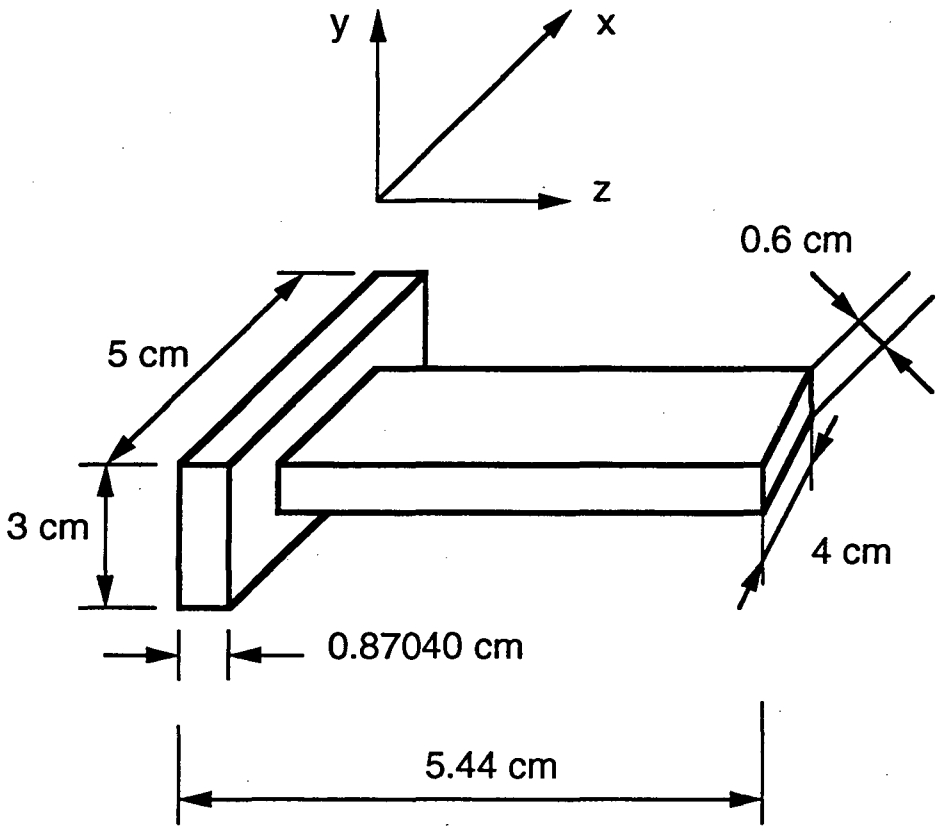

Fig. 3

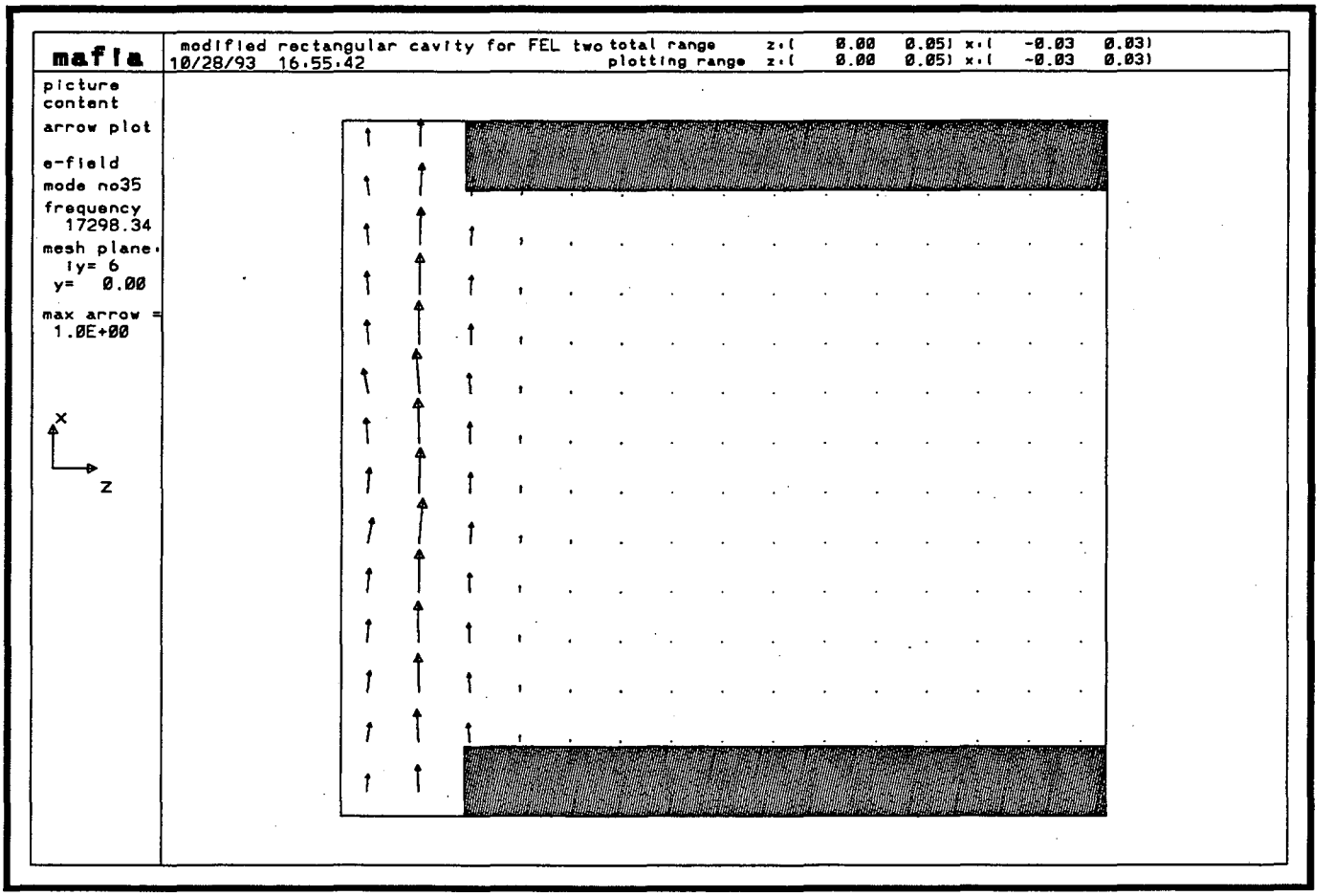
mafia
modified rectangular cavity for FEL two
10/28/93 16.55.42
total range z:(0.00 0.05) x:(-0.03 0.03)
plotting range z:(0.00 0.05) x:(-0.03 0.03)
picture content
arrow plot
e-field
mode no35
frequency
17298.34
mesh plane
iy= 6
y= 0.00
max arrow =
1.0E+00
x
z

Fig. 4

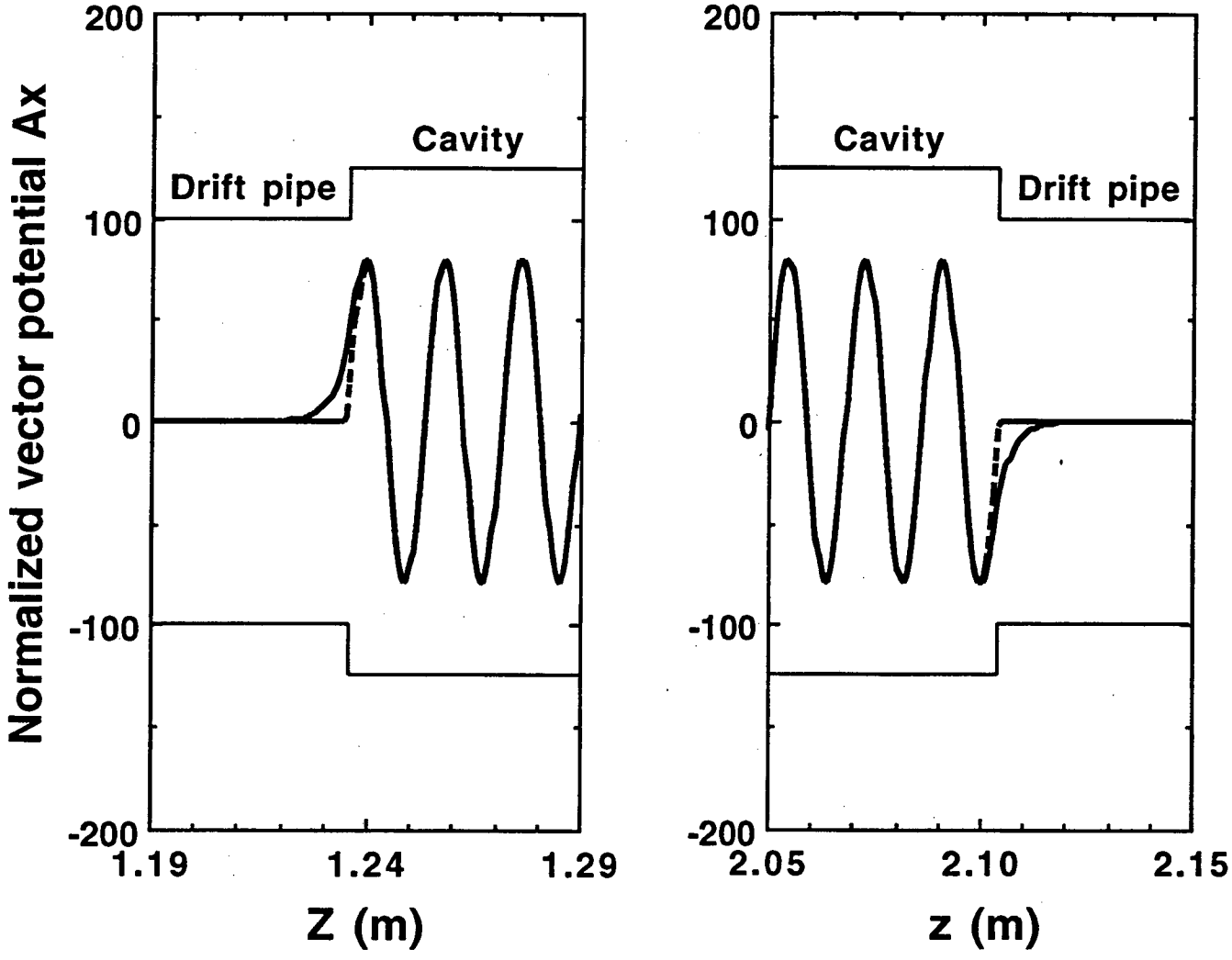
Normalized vector potential Ax
200
100
0
-100
-200
Cavity
Drift pipe
1.19
1.24
1.29
Z (m)
Cavity
Drift pipe
2.05
2.10
2.15
z (m)

Fig. 5

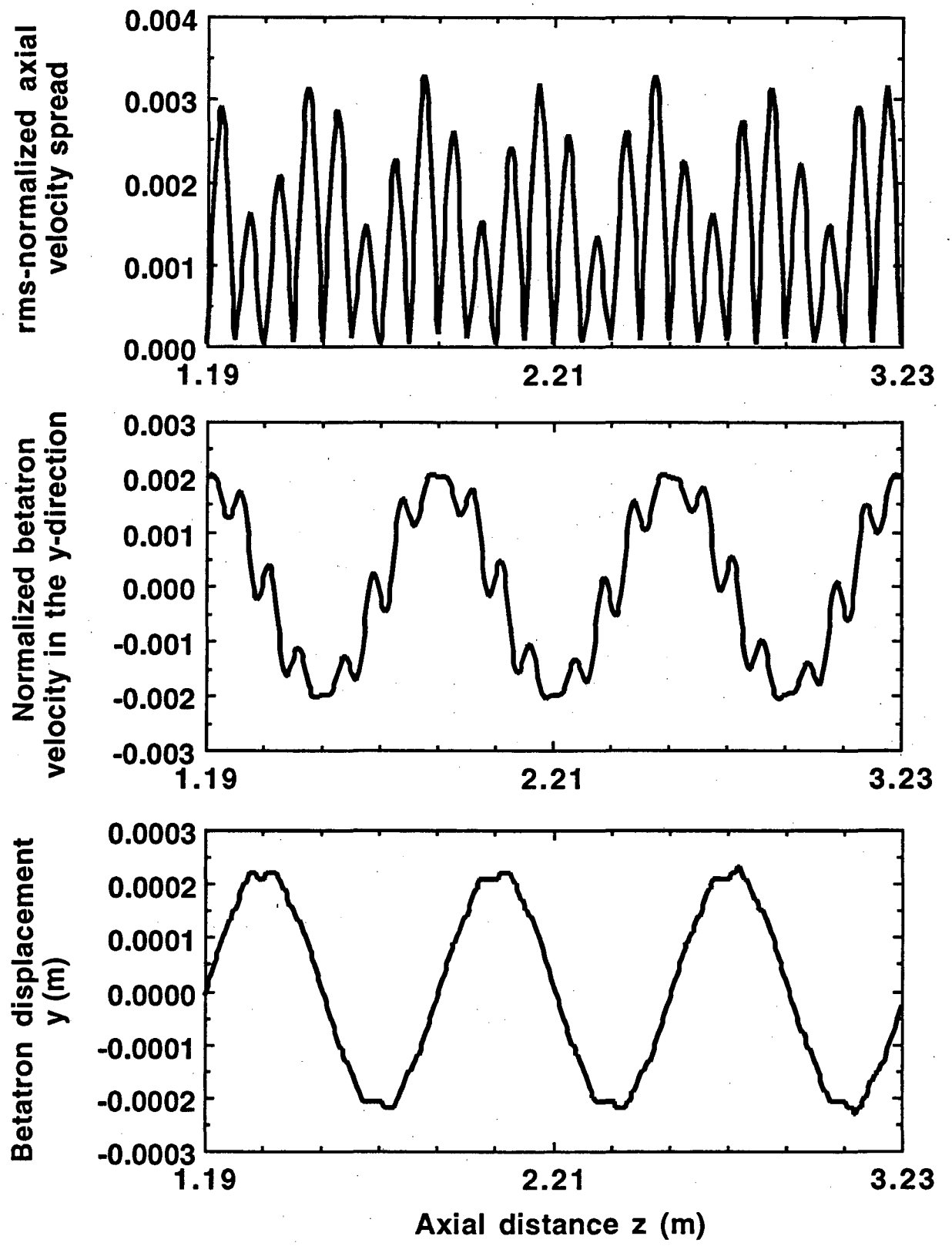
rms-normalized axial velocity spread
0.004
0.003
0.002
0.001
0.000
1.19
2.21
3.23
Normalized betatron velocity in the y-direction
0.003
0.002
0.001
0.000
-0.001
-0.002
-0.003
1.19
2.21
3.23
Betatron displacement y (m)
0.0003
0.0002
0.0001
0.0000
-0.0001
-0.0002
-0.0003
1.19
2.21
3.23
Axial distance z (m)

Fig. 6

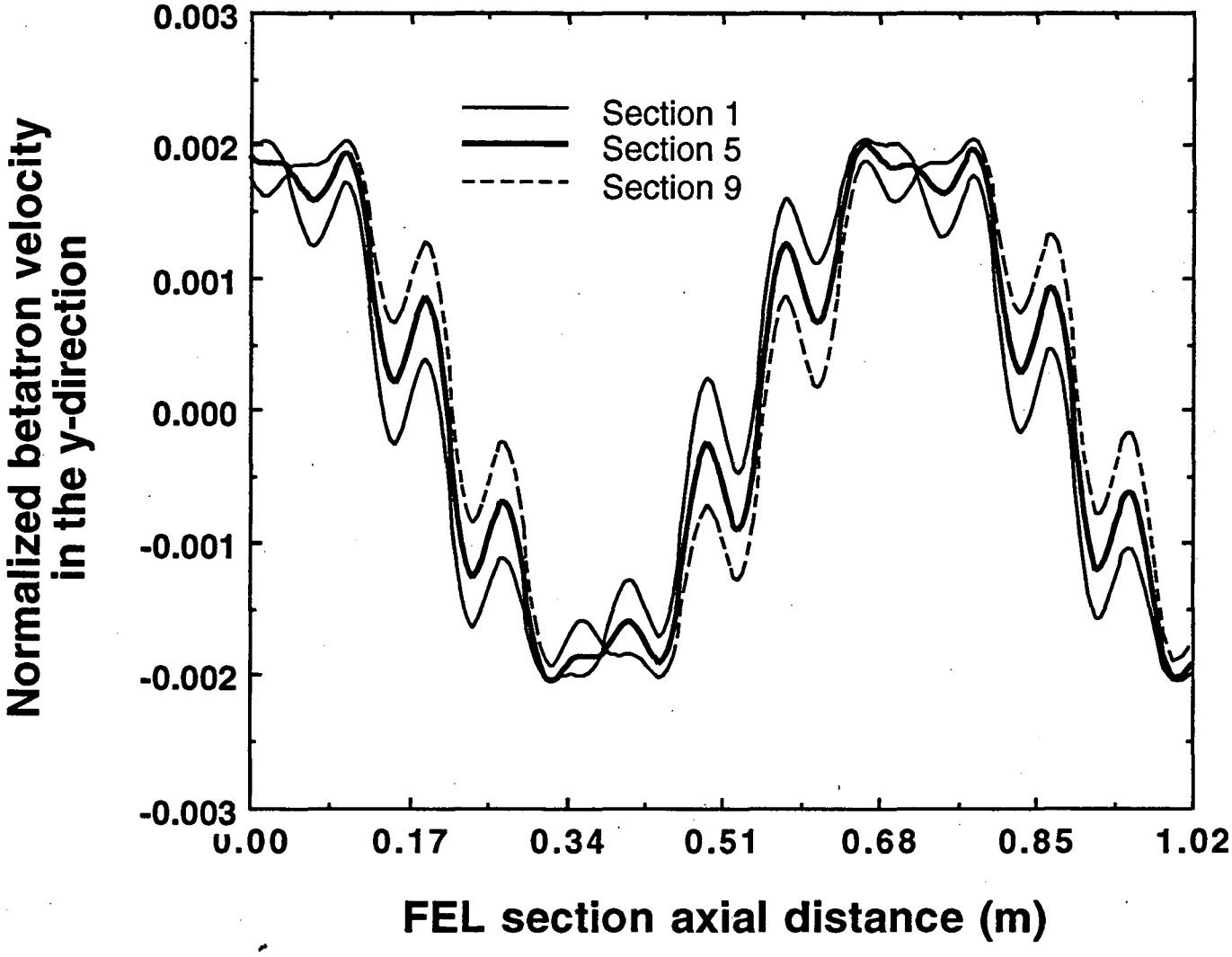
Normalized betatron velocity in the y-direction
0.003
0.002
0.001
0.000
-0.001
-0.002
-0.003
Section 1
Section 5
Section 9
0.00
0.17
0.34
0.51
0.68
0.85
1.02
FEL section axial distance (m)

Fig. 7

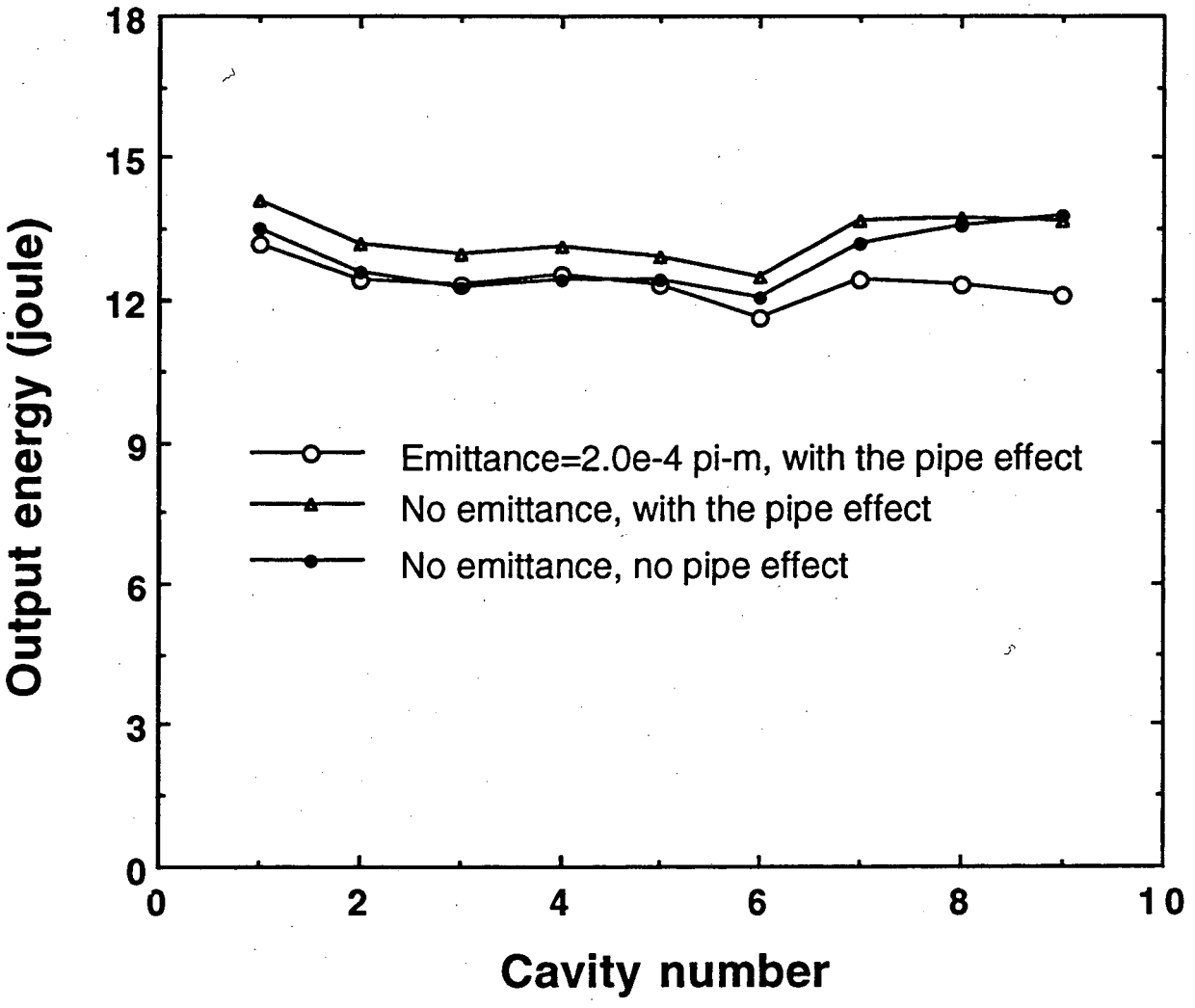
Output energy (joule)
18
15
12
9
6
3
0
0
2
4
6
8
10
Cavity number
Emittance=2.0e-4 pi-m, with the pipe effect
No emittance, with the pipe effect
No emittance, no pipe effect

Fig. 8

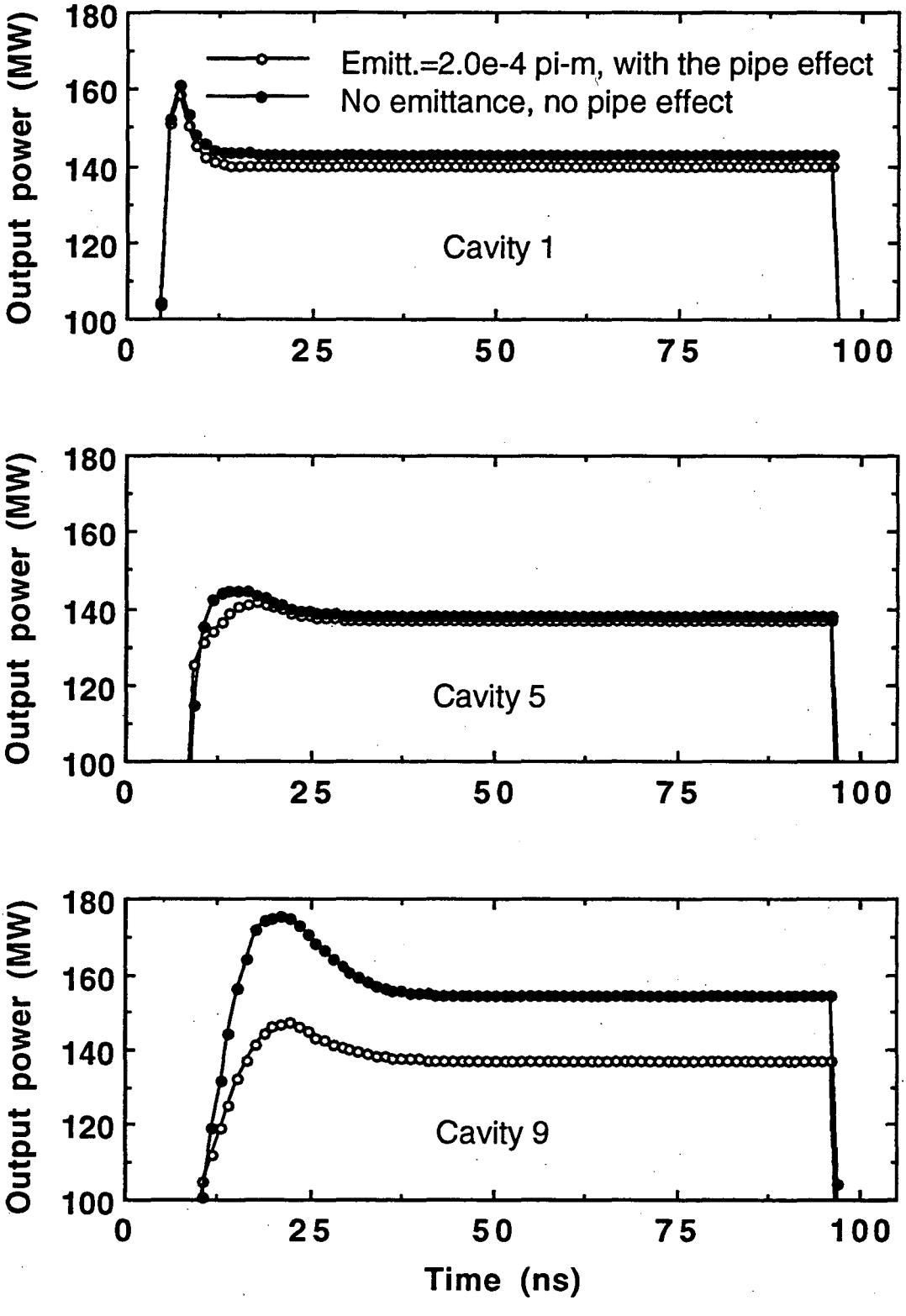
Output power (MW)
180
160
140
120
100
0
25
50
75
100
Emitt.=2.0e-4 pi-m, with the pipe effect
No emittance, no pipe effect
Cavity 1
Cavity 5
Cavity 9
Time (ns)

Fig. 9

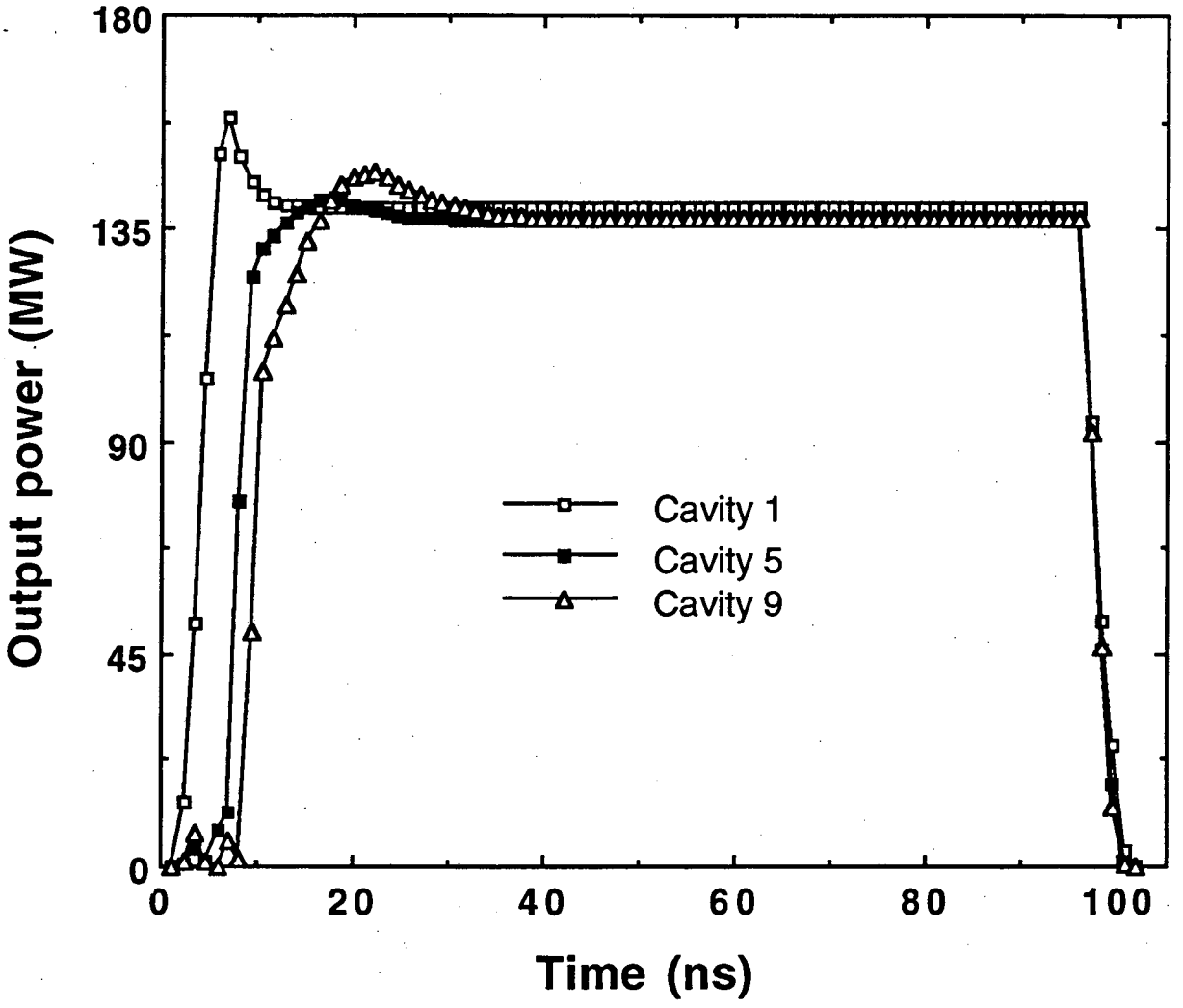
180
135
90
45
0
Output power (MW)
0
20
40
60
80
100
Time (ns)
Cavity 1
Cavity 5
Cavity 9

Fig. 10

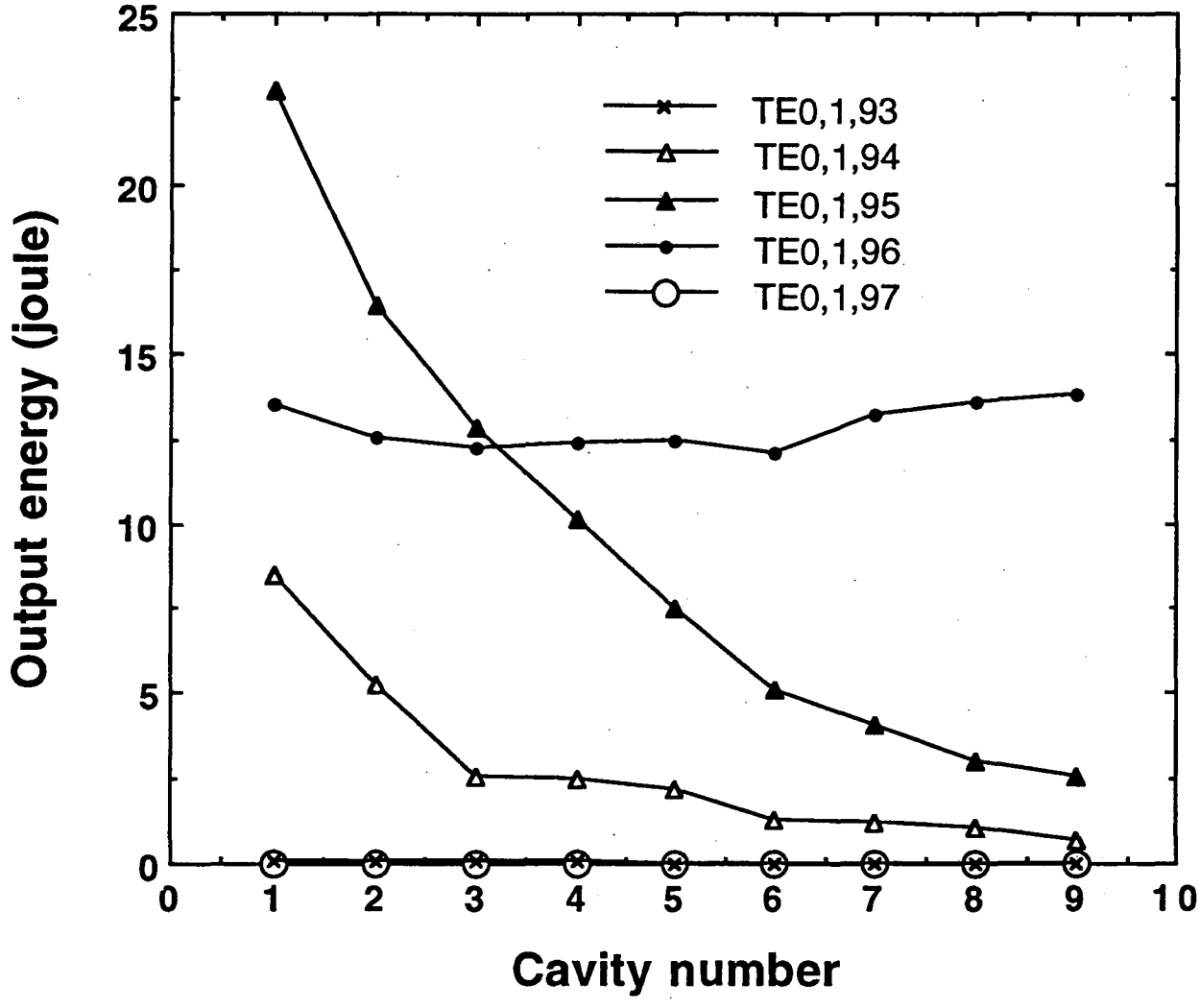
25
20
15
10
5
0
0
1
2
3
4
5
6
7
8
9
10
Output energy (joule)
Cavity number
TE0,1,93
TE0,1,94
TE0,1,95
TE0,1,96
TE0,1,97

Fig. 11

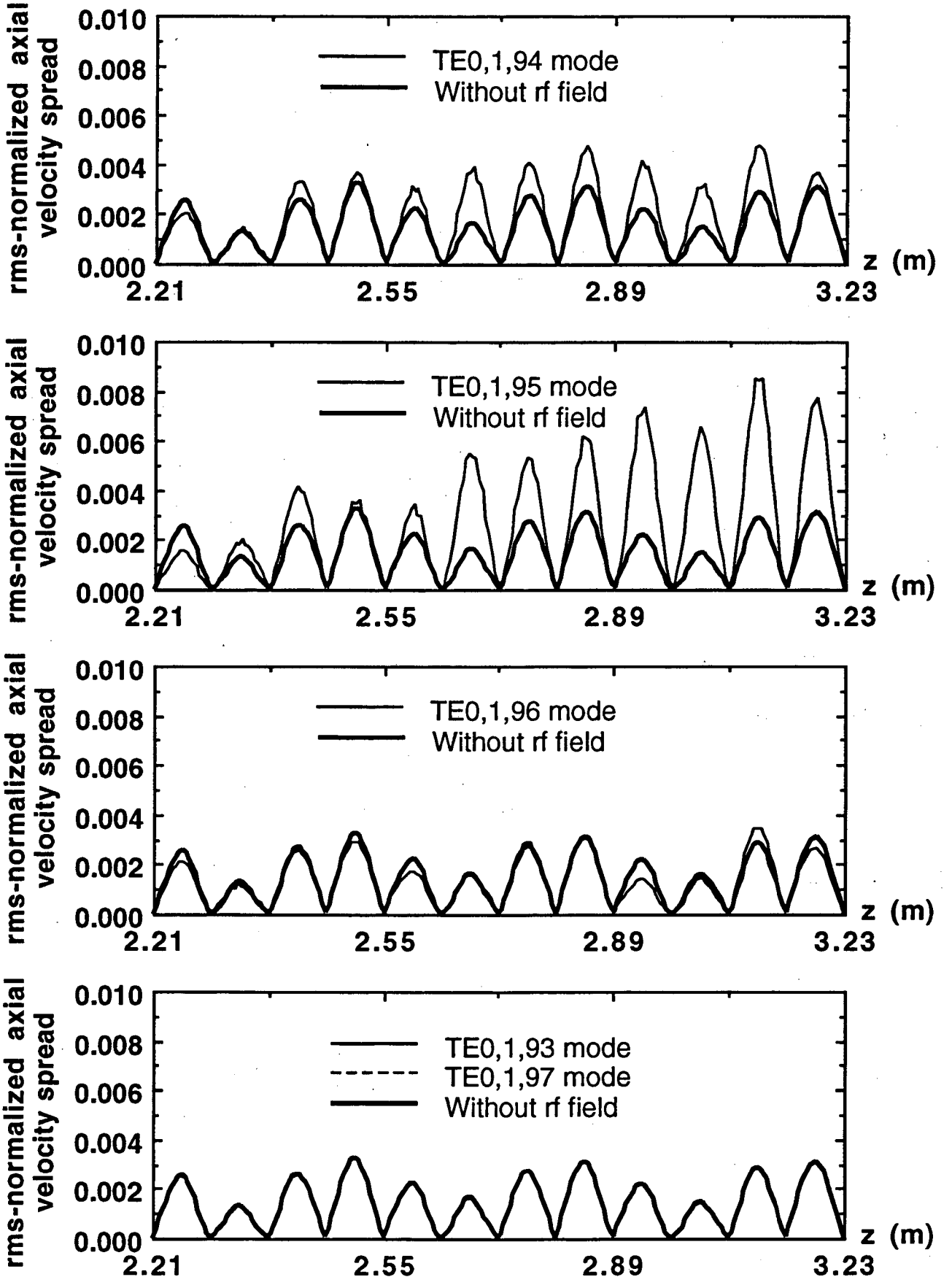
rms-normalized axial velocity spread
0.010
0.008
0.006
0.004
0.002
0.000
2.21
2.55
2.89
3.23
z (m)
TE0,1,94 mode
Without rf field
TE0,1,95 mode
Without rf field
TE0,1,96 mode
Without rf field
TE0,1,93 mode
TE0,1,97 mode
Without rf field

Fig. 12

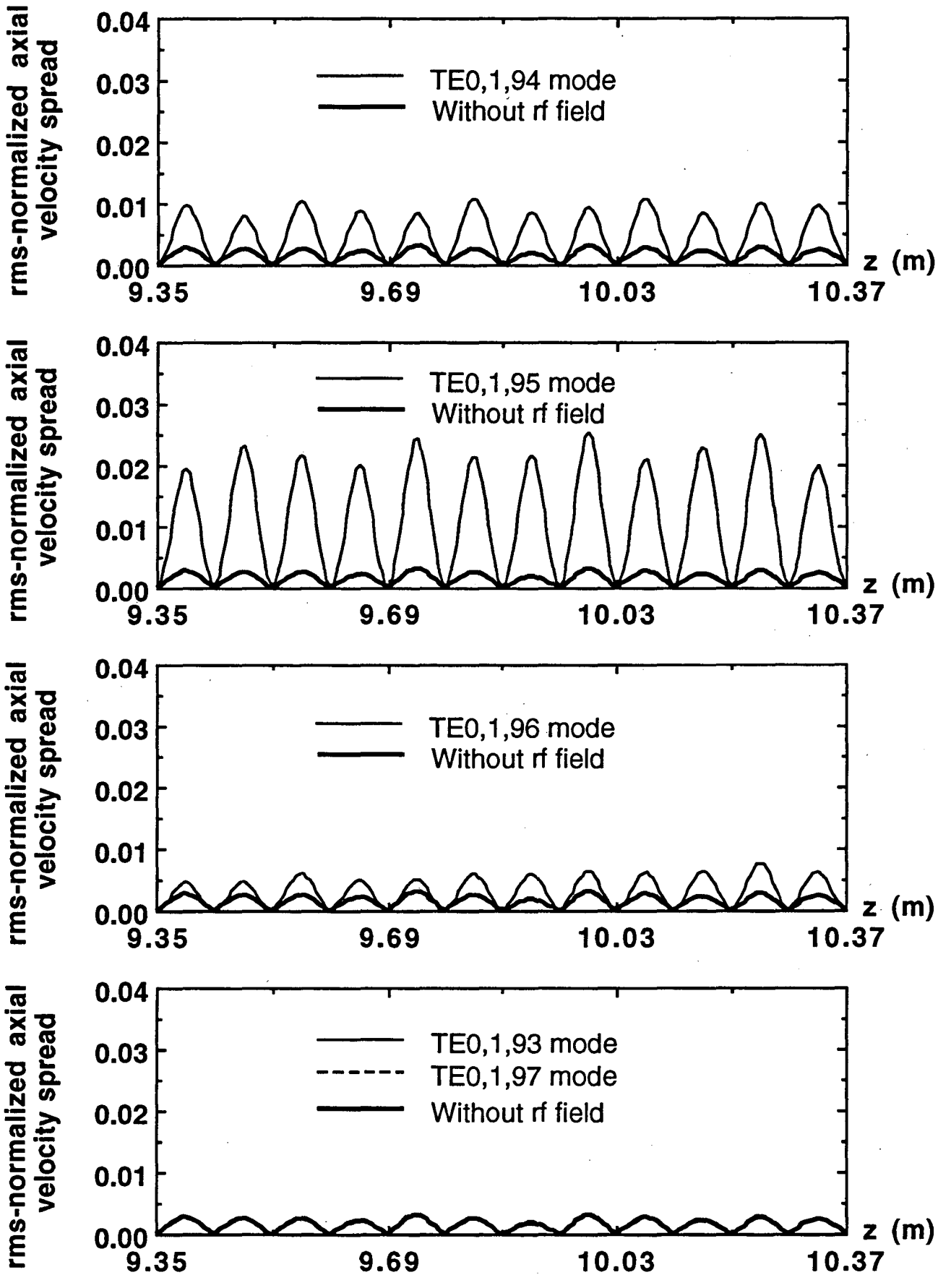
rms-normalized axial velocity spread
0.04
0.03
0.02
0.01
0.00
9.35
9.69
10.03
10.37
z (m)
TE0,1,94 mode
Without rf field
TE0,1,95 mode
Without rf field
TE0,1,96 mode
Without rf field
TE0,1,93 mode
TE0,1,97 mode
Without rf field

Fig. 13

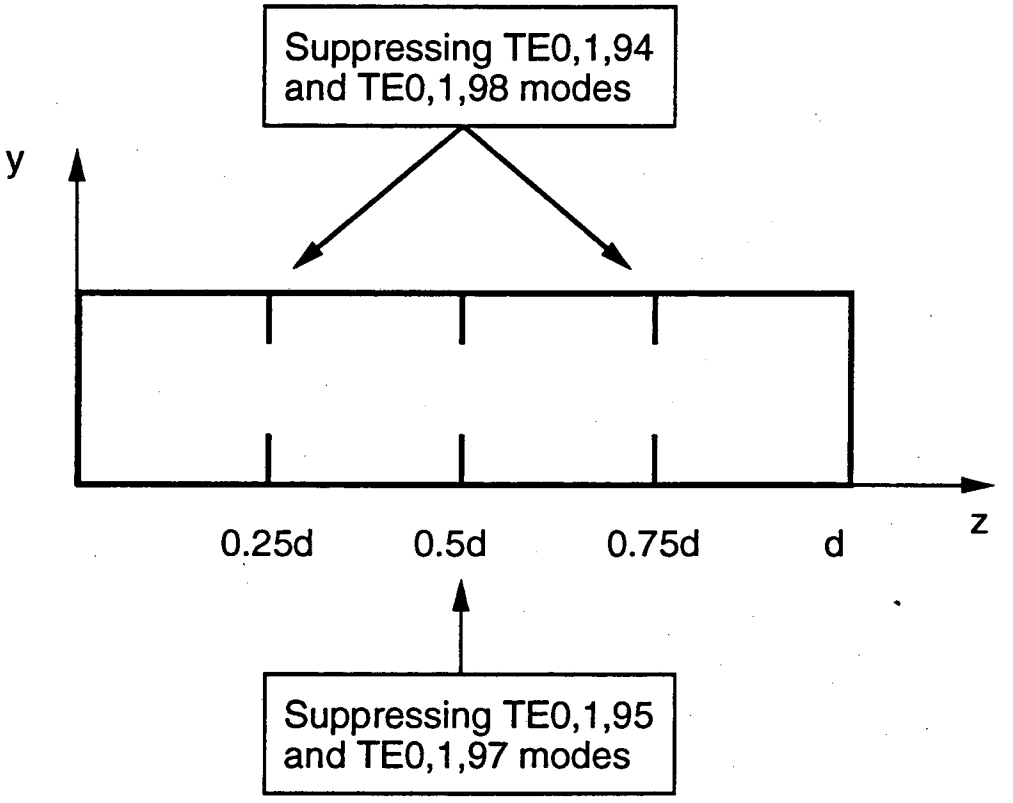
Suppressing TE0,1,94
and TE0,1,98 modes
y
z
0.25d
0.5d
0.75d
d
Suppressing TE0,1,95
and TE0,1,97 modes

Fig. 14

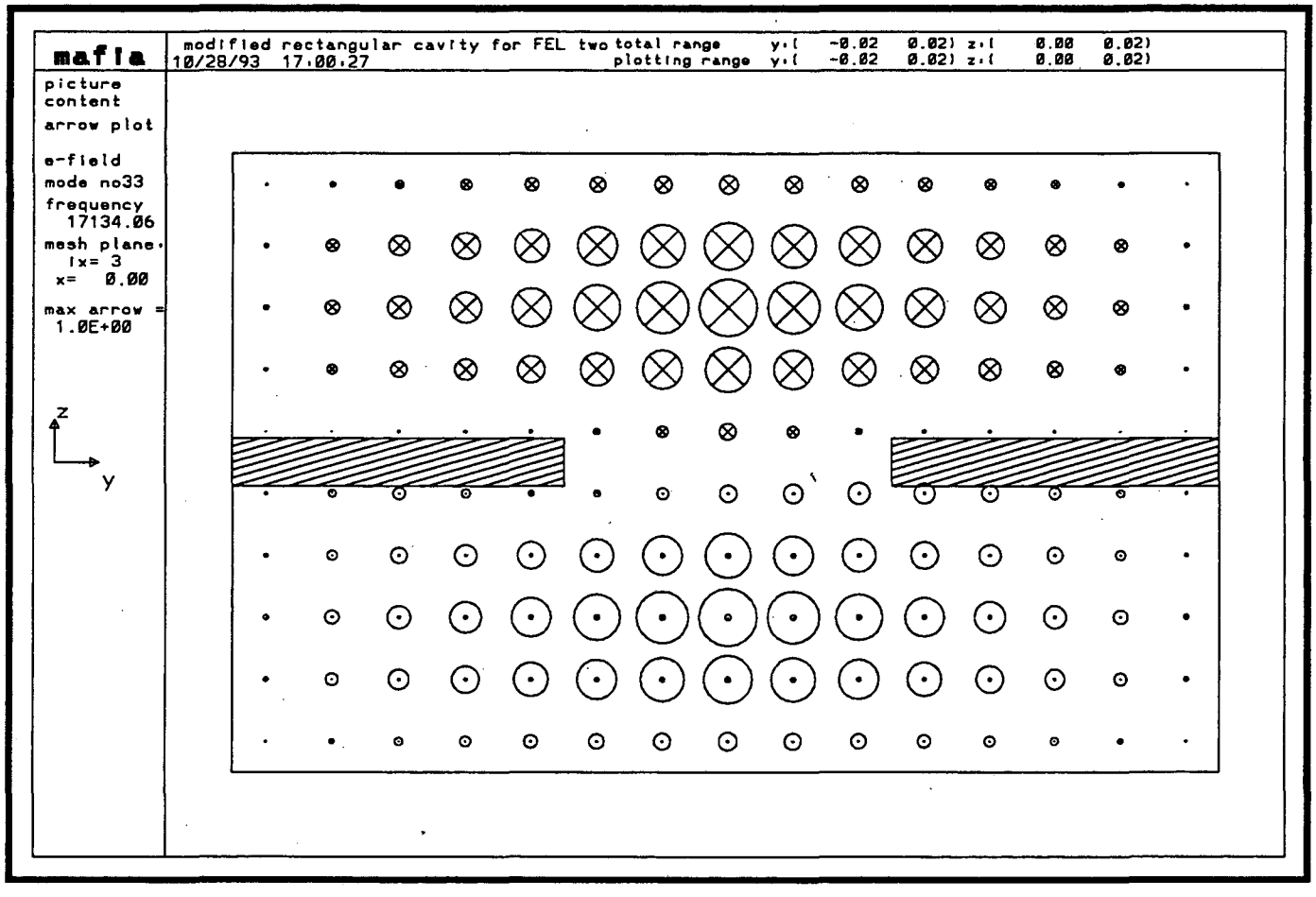
mafia
modified rectangular cavity for FEL two total range y:(-0.02 0.02) z:(0.00 0.02)
10/28/93 17:00:27 plotting range y:(-0.02 0.02) z:(0.00 0.02)
picture content
arrow plot
e-field
mode no33
frequency 17134.06
mesh plane
ix= 3
x= 0.00
max arrow = 1.0E+00
z
y

LAWRENCE BERKELEY LABORATORY
UNIVERSITY OF CALIFORNIA
TECHNICAL INFORMATION DEPARTMENT
BERKELEY, CALIFORNIA 94720